Altered APP Processing in PDAPP (Val717 → Phe) Transgenic Mice Yields Extended-Length Aβ Peptides†

Chera Esh,‡ Lyle Patton,‡ Walter Kalback,‡ Tyler A. Kokjohn,‡,§ John Lopez,|| Daniel Brune,|| Amanda J. Newell,⊥ Thomas Beach,⊥ Dale Schenk,# Dora Games,# Steven Paul,¶ Kelly Bales,¶ Bernardino Ghetti,£ Eduardo M. Castaño,@ and Alex E. Roher*,‡

The Longtine Center for Molecular Biology and Genetics, Sun Health Research Institute, Sun City, Arizona 85351, Department of Microbiology, Midwestern University, Glendale, Arizona 85308, Department of Chemistry and Biochemistry, Arizona State University, Tempe, Arizona 85287, W. Harold Civin Laboratory of Neuropathology, Sun Health Research Institute, Sun City, Arizona 85351, Elan Pharmaceuticals, South San Francisco, California 94080, Neuroscience Discovery Research, Lilly Research Laboratories, Eli Lilly and Company, Indianapolis, Indiana 46285, Indiana Alzheimer's Disease Center, Indianapolis, Indiana 46202, and Fundacion Instituto Leloir, Buenos Aires, Argentina C1405BWE

Received June 23, 2005; Revised Manuscript Received August 12, 2005

ABSTRACT: Central to the pathology of Alzheimer's disease (AD) is the profuse accumulation of amyloid-β (Aβ) peptides in the brain of affected individuals, and several amyloid precursor protein (APP) transgenic (Tg) mice models have been created to mimic Aβ deposition. Among these, the PDAPP Tg mice carrying the familial AD APP 717 Val → Phe mutation have been widely used to test potential AD therapeutic interventions including active and passive anti-Aβ immunizations. The structure and biochemistry of the PDAPP Tg mice Aβ-related peptides were investigated using acid and detergent lysis of brain tissue, ultracentrifugation, FPLC, HPLC, enzymatic and chemical cleavage of peptides, Western blot, immunoprecipitation, and MALDI−TOF and SELDI−TOF mass spectrometry. Our experiments reveal that PDAPP mice produce a variety of C-terminally elongated Aβ peptides in addition to Aβ $n-40$ and Aβ $n-42$, as well as N-terminally truncated peptides, suggesting anomalous proteolysis of both APP and Aβ. Important alterations in the overall APP degradation also occur in this model, resulting in a striking comparative lack of CT83 and CT99 fragments, which may be inherent to the strain of mice, a generalized γ-secretase failure, or the ultimate manifestation of the overwhelming amount of expressed human transgene; these alterations are not observed in other strains of APP Tg mice or in sporadic AD. Understanding at the molecular level the nature of these important animal models will permit a better understanding of therapeutic interventions directed to prevent, delay, or reverse the ravages of sporadic AD.

Alzheimer's disease (AD)[1] presently affects an estimated 4 million elderly individuals in the U.S.A. This neurodegenerative disorder strikes 4% of individuals at 65 years of age and nearly 50% of those at age 85, with an annual cost of about 80 billion dollars. Moreover, the average life expectancy has increased from 50 years in 1900 to almost 80 years in 2004, leading to a projected quadruple in the number of AD cases by the year 2050 (*1*). Therefore, there is an urgent need for effective therapeutic interventions that may prevent AD, delay its onset, or alter the course of this dementia.

The deposition of amyloid-β (Aβ) peptides in the brains of patients with AD has been the object of intense research since the seminal publications of Glenner and Wong and Masters et al. describing its isolation and amino acid sequence (*2*, *3*). The profuse accumulation of Aβ peptides in the AD brain parenchyma and vasculature, a universal condition of all forms of this disease whether familial or sporadic, was integrated into the amyloid cascade hypothesis

† This research was supported by the NIA Grants AG-19795 and AG-17490, the NIA-ADCC (AG-19610 and AG-10133), and the State of Arizona Alzheimer's Research Center.

* To whom correspondence should be addressed: Sun Health Research Institute, 10515 W. Santa Fe Dr., Sun City, AZ 85351. Telephone: (623) 876−5465. Fax: (623) 876-5698. E-mail: alex.roher@sunhealth.org.

‡ The Longtine Center for Molecular Biology and Genetics, Sun Health Research Institute.

§ Midwestern University.

|| Arizona State University.

⊥ W. Harold Civin Laboratory of Neuropathology, Sun Health Research Institute.

Elan Pharmaceuticals.

¶ Eli Lilly and Company.

£ Indiana Alzheimer's Disease Center.

@ Fundacion Instituto Leloir.

[1] Abbreviations: AD, Alzheimer's disease; Aβ, amyloid-β; APP, amyloid precursor protein; Arg, arginine; Asp, aspartic acid; BBB, blood brain barrier; BCA, bicinchoninic acid; CHCA, α-cyano-4-hydroxycinnamic acid; CNBr, cyanogen bromide; CT, carboxy terminal; DTT, dithiothreitol; EDTA, ethylenediaminetetraacetate acid; F, Phe, phenylalanine; FAD, familial Alzheimer's disease; FPLC, fast protein liquid chromatography; GDFA, glass-distilled formic acid; Gly, glycine; HPLC, high-performance liquid chromatography; HRP, horseradish peroxidase; IP, immunoprecipitation; Iso, isomerized; LDS, lithium dodecyl sulfate; Lys, lysine; MALDI−TOF, matrix-assisted laser desorption/ionization−time-of-flight; Met, methionine; M_r, relative molecular mass; MW, molecular weight; ND, nondemented; NFT, neurofibrillary tangles; PBS, phosphate-buffered saline; PDAPP, platelet-derived amyloid precursor protein; PDGF, platelet-derived growth factor; PS, presenilin; RPC, reverse-phase chromatography; RT, room temperature; SDS, sodium dodecyl sulfate; SELDI−TOF, surface-enhanced laser desorption/ionization−time-of-flight; Ser, serine; TFA, trifluoroacetic acid; Thr, threonine; Thy, thymus cell antigen-1; TPCK, L-tosylamido-2-phenylethyl chloromethyl ketone; Tg, transgenic; Tris-HCl, tris(hydroxymethyl)aminomethane hydrochloride; V, Val, valine.

10.1021/bi051213+ CCC: $30.25
Published on Web 09/29/2005

as the central causative factor in the pathogenesis of the AD dementia (*4*, *5*).

In an attempt to reproduce AD neuropathology, several transgenic (Tg) mouse strains have been engineered to express combinations of human familial AD (FAD) mutant genes. These Tg mice are widely utilized in academic, pharmaceutical, and biotechnological laboratories to test the efficacy of diverse compounds and strategies intended to mitigate the deleterious effects of Aβ peptide accumulation or to aid amyloid deposit clearance. Included in this group are inhibitors of the β- and γ-secretase activity, substances that interfere with Aβ aggregation, anti-Aβ antibodies, anti-inflammatory compounds, cholesterol metabolism modulators, antioxidants, neuroprotective and neurotrophic agents, and metal ion chelators. In addition, several amyloid-tagging chemicals that may help in the early diagnosis of AD are also being tested in the Tg mouse models.

It has been assumed that the amyloid precursor protein (APP) and the APP/presenilin-1 (APP/PS1) Tg mouse models replicate the human AD amyloid cascade. This hypothesis is based on the observations that the Tg mice generate morphologically similar amyloid plaque deposits that contain the expected Aβ40/42 antigenic determinants as revealed by standard amyloid peptide immunoassays. However, given the clear results obtained to date from studies of a few Tg mice strains (*6*−*10*), whether the new multiple FAD mutation-expressing animals will replicate human AD or even produce the identical amyloid species found in demented humans is uncertain. Thorough chemical characterization is essential to understand how Tg mice AD models actually compare to humans because unrecognized biochemical discrepancies might foster erroneous experimental inferences. Our initial studies have demonstrated that the amyloid deposited in Tg mice expressing singly mutant FAD APP genes (APP23 and tg2576) is physically and chemically distinct from amyloid deposits characteristic of human sporadic AD (*11*).

Physicochemical differences in Tg mouse and AD patient amyloid could influence both the outcome and interpretation of therapeutic protocols intended to prevent or remove amyloid deposits. For example, active vaccination of Tg mice with amyloid peptides has resulted in the dramatic disappearance of parenchymal amyloid deposits and an apparent improvement in cognitive function in these animals (*12*, *13*). Examination of Aβ-immunized AD patient brains also demonstrated a localized and patchy decrease in the number of parenchymal plaques (*14*−*16*) and slower cognitive decline in persons expressing a significant titer of circulating anti-Aβ antibodies (*17*). A single dose of monoclonal antibody against Aβ reduced memory deficits in the PDAPP Tg mice without altering brain Aβ levels (*18*), while chronic administration, in addition to memory improvement, decreased the amyloid burden of the rodent (*19*, *20*). However, mouse vaccination may yield much better results than could ever be attained in AD patients because mouse plaque amyloid is more readily disrupted (*9*, *11*). Initial examinations of vaccinated Tg mice reveal the counterintuitive findings that, while parenchymal amyloid plaques partially disappear, total Aβ peptide levels remain unaltered and APP processing continues unabated (*21*, *22*). Given that AD intervention may need to be undertaken early in the disease course, questions arise over the potential long-term effects of large pools of uncleared soluble and possibly quite toxic amyloid species (*23*). Biochemical analyses and comparisons between multiple Tg animals, immunized and unimmunized, to human AD patients will help elucidate which models are the best AD mimics. They will clarify the response to amyloid immunotherapy, define the extent to which uncleared soluble amyloid persists in immunized humans, and aid the development of more effective therapeutic interventions.

In the present study, we have characterized the APP and Aβ peptides produced by PDAPP Tg mice carrying the FAD APP Val → Phe mutation at position 717 (*24*). This amyloid cascade model generates, besides Aβ ending at residues 40 and 42, extended-length Aβ peptides organized into abundant flocculent deposits, as well as a smaller number of amyloid core plaques that stain with thioflavine-S. In addition, PDAPP mice exhibit a different pattern of APP degradation than that observed in sporadic AD and human FAD carrying the V717F mutant (*25*).

EXPERIMENTAL PROCEDURES

Frozen brains from 60 PDAPP Tg mice, 16−20 months of age, were kindly provided by Elan Pharmaceuticals, South San Francisco, CA, and Eli Lilly, Indianapolis, IN. A total of 16 additional PDAPP Tg mice brains were generously donated by Dr. Lennart Mucke, The Gladstone Institute, University of California at San Francisco. The latter PDAPP Tg mice brains corresponded to the line H6 described by Mucke et al. (*26*). The PDAPP mice express the human APP with the Val → Phe mutation at position 717 (APP_{770} isoform notation), under the control of the platelet-derived growth factor (PDGF) promoter. To estimate the number of deposits, their distribution, and the total proportion of core plaques and diffuse amyloid deposits, frozen sagital sections were made and stained with the Campbell−Switzer silver stain and thioflavine-S.

Isolation of Amyloid. The brain hemispheres from 12 PDAPP Tg mice, from which the cerebellum and brain stem were excised, were minced and suspended in 120 mL of 50 mM Tris-HCl buffer at pH 7.5 containing 4 mM EDTA and 5% SDS. After 24 h of gentle stirring, the suspension was filtered through a 150 μm nylon mesh to remove large insoluble blood vessels and the filtrate was centrifuged at 285000*g* in a SW 41 rotor (Beckman, Fullerton, CA) for 2 h at 20 °C. The small pellets were then suspended in a total of 6 mL of distilled water and sieved through a 45 μm nylon mesh. Aliquots of 1 mL of the filtrate were submitted to a discontinuous sucrose gradient formed by layering 2 mL each of 2.0, 1.7, 1.5, 1.3, 1.2, and 1.0 M sucrose solutions (Fluka, St Louis, MO) prepared in 50 mM Tris-HCl at pH 7.5 and 0.1% SDS, into 12 mL transparent polycarbonate tubes (Beckman, Fullerton, CA) and centrifuged at 150000*g* for 1 h at 20 °C in a Beckman SW41 rotor. The different layers were harvested by suction using a peristaltic pump (LKB, Bromma, Sweden), and the sucrose was removed after dilution with Tris buffer by high-speed centrifugation as described above. In a parallel experiment, 2 g of frontal cerebral cortex from an individual carrying the FAD V717F were processed following the same procedure employed for the isolation of the insoluble amyloid cores from the PDAPP Tg mice.

Isolation of Total Aβ Peptides. Approximately 3 g of mouse brain tissue, from which the cerebellum and brain

stem were removed, was homogenized in 20 mL of 90% glass-distilled formic acid (GDFA). After incubation for 15 min at room temperature (RT), the lysed tissue was centrifuged at 285000*g* in a Beckman SW41 rotor for 1 h at 10 °C. The clear supernatant was collected, avoiding the surface lipid layer and small insoluble pellet, and divided into 500 μL aliquots, which were immediately stored at −86 °C. These samples were submitted to fast protein liquid chromatography (FPLC) on a Superose 12 size-exclusion column (10 × 300 mm, Amersham Pharmacia, Piscataway, NJ). The column was equilibrated, and the chromatography was developed at RT in 80% GDFA at a flow rate of 15 mL/h. The eluate absorbance was monitored at 280 nm. The column elution profile was determined by running an analogous M_r peptide with the reverse Aβ (42−1) amino acid sequence. The 3−8-kDa-containing fractions were collected and pooled, and the GDFA volume was immediately reduced to ∼10 μL by vacuum centrifugation (Savant, Holbrook, NY) and stored at −86 °C.

High-Performance Liquid Chromatography (HPLC) Purification of Aβ Peptides. The FPLC fractions containing the 3−8-kDa molecules were further purified by reverse-phase HPLC. Five FPLC runs were pooled and concentrated to 50 μL. A total of 200 μL of 90% GDFA was added, and the final volume was adjusted to 500 μL with distilled water. The specimens were loaded onto a reverse-phase Zorbax SB-C8 column (4.6 × 250 mm, Mac-Mod, Chadds Ford, PA) equilibrated with 20% acetonitrile/80% water and 0.1% trifluoroacetic acid (TFA). Separations were performed using a linear (20−40%) acetonitrile gradient developed for a period of 60 min at 80 °C and 1 mL/min flow rate. Column eluate was monitored by following UV absorbance at 214 nm.

Tryptic Hydrolysis, Cyanogen Bromide (CNBr) Cleavage, and Separation of Aβ Peptides. The peptide samples separated by reverse-phase HPLC were reduced to a volume of ∼20 μL, and 80% GDFA was added to yield a final sample size of 1 mL. They were then dialyzed (1000-Da cutoff, SpectraPor 6, Rancho Dominguez, CA), once against 2 L of distilled water and 3 times in 2 L of 100 mM ammonium bicarbonate. The dialyzed Aβ peptides were digested with TPCK-treated trypsin (10 μg/specimen, Worthington Biochemicals Corp., Lakewood, NJ) for 16 h at 37 °C. The resulting tryptic peptides were lyophilized and dissolved in 500 μL of 80% GDFA followed by the addition of a small crystal of CNBr, thoroughly mixed, and incubated for 16 h at RT. The volume was reduced to ∼20 μL by vacuum centrifugation and distilled water containing 0.1% TFA added to yield a final volume of 500 μL. The tryptic and CNBr-cleaved peptides derived from the HPLC fractions 2, 3, and 4 were further purified by HPLC on a reverse-phase Discovery Bio-wide pore C18 column (4.6 × 150 mm, 3 μm beads, Supelco, Bellefonte, PA). The chromatography was developed at 60 °C with a linear gradient of 0−40% acetonitrile and 0.1% TFA at a flow rate of 0.4 mL/min for a period of 180 min. Eluate absorbance was monitored at 214 nm.

MALDI−TOF Mass Spectrometry of Aβ Peptides. Spectrometric data were obtained using a MALDI−TOF Voyager DE STR mass spectrometer equipped with a nitrogen laser that produced 337 nm pulses of 3 ns duration at a repetition rate of 20 Hz. Mass spectra were acquired in the positive-ion mode using delayed extraction and a reflectron. HPLC-purified peptide samples were dried, dissolved in a small volume of 50% aqueous acetonitrile containing 0.1% TFA, and then mixed with an equal volume of a saturated solution of α-cyano-4-hydroxycinnamic acid (CHCA) dissolved in the same solvent. Aliquots (1 μL) of the mixture were dried on a stainless steel sample plate, and a mass spectrum for each sample was obtained as the average from 100 laser shots. Calibration was performed using CalMix 2 from Applied Biosystems (Foster City, CA) as an external standard. CalMix 2 is a mixture of the following polypeptides (singly protonated monoisotopic masses in parentheses): angiotensin1 (1296.685), ACTH clip 1−17 (2093.087), ACTH clip 18−39 (2465.199), ACTH clip 7−38 (3657.929), and bovine insulin (5730.609). Monoisotopic masses obtained by this procedure are typically accurate to within <0.1 Da over the mass range of peptides examined in this work. Because carbon occurs naturally as an isotopic mixture of roughly 99% C-12 and 1% C-13 and the peptides analyzed contain a large number of carbon atoms, each type of peptide produces a cluster of peaks differing in mass by 1 Da. The lowest molecular mass peak is composed of C-12 and the lowest mass isotopes of nitrogen, hydrogen, oxygen, and, if present, sulfur. The centroid mass for this peak is the monoisotopic mass of the peptide and was obtained for the peptides examined using deisotoping software that is part of the Data Explorer analysis program.

SELDI−TOF Mass Spectrometry of Aβ Peptides. Selected HPLC peaks were dialyzed with 1000 MW cutoff bags against 50 mM Tris-HCl at pH 8, followed by 10 mM Tris-HCl at pH 8. The dialyzed peak samples were analyzed using SELDI−TOF (surface-enhanced laser desorption/ionization−time-of-flight) mass spectrometry (Ciphergen Biosystems, Freemont, CA). The monoclonal antibodies 6E10 and 4G8 (Signet, Dedham, MA) and polyclonal R293 and R306 antibodies raised against the C-terminal region of Aβ 40 and Aβ 42, respectively (kindly donated by Dr. Pankaj Mehta) and bovine IgG (Pierce, Rockford, IL), as a negative control, were adjusted to a concentration of 0.5 mg/mL in PBS, loaded (2 μL) onto PS20 ProteinChip Arrays, and incubated in a humidity chamber for 1 h at RT. The chip surfaces were blocked with 3 μL of ethanolamine (1 M, pH 8) for 30 min. After the solutions were removed, the spots were washed with 50 mM Tris-HCl at pH 8 (5 μL) for 5 min. The chips were washed in 15 mL Falcon tubes 2 times with 10 mL of PBS and 0.5% (v/v) Triton X-100 for 10 min, 2 times with 10 mL of PBS for 10 min, and then rinsed with 10 mL distilled water. The protein chips were loaded into a Bioprocessor (Ciphergen Biosystems, Fremont, CA), and 10 μL samples were loaded and incubated in a humidity chamber for 2 h at RT. Synthetic Aβ 40 and 42 peptide standards (California Peptide Research, Napa, CA) were used as positive controls, and 2% fetal bovine serum (Sigma, St. Louis, MO) diluted in PBS served as a negative control. After the binding medium was removed, the chips were washed 2 times with 250 μL PBS and 0.5% (v/v) Triton X-100 per spot for 10 min and then 2 times with 250 μL of PBS per spot for 10 min. After a wash with distilled water (2 times 10 min each), the chips were air-dried. A 1:5 dilution of saturated CHCA in 50% acetonitrile and 50% of 1% TFA was applied (1 μL) 2 times, and mass assignments were made by 100 averaged shots in a Ciphergen SELDI Protein Biology

System II. Calibration was made externally using the Ciphergen all-in-1 peptide standard.

Western Blotting. The Tg mice brain tissue was homogenized in 10 volumes PBS at pH 7.4 containing complete Protease Inhibitor Cocktail (Roche Diagnostics, Mannheim, Germany). Total protein concentrations were determined using the BCA protein assay kit (Pierce, Rockford, IL). Samples were diluted into NuPage LDS sample buffer (Invitrogen, Carlsbad, CA) containing 50 mM dithiothreitol (DTT) and 10% SDS and heated for 10 min at 80 °C, and equal amounts of total protein were loaded onto 4−12% Bis-Tris gels (Invitrogen, Carlsbad, CA) and electrophoresed using NuPage MES running buffer. Kaleidoscope prestained protein molecular mass standards (Bio-Rad, Hercules, CA) were loaded onto each gel. Proteins were transferred onto nitrocellulose membranes (Invitrogen, Carlsbad, CA) using NuPage transfer buffer containing 20% methanol. The membranes were blocked in 5% nonfat dry milk in PBS and 0.05% (v/v) Tween 20 (Fluka, St. Louis, MO). All of the following primary and secondary antibodies were diluted in blocking buffer. Carboxy-terminal proteins were detected with a 1:1500 dilution of an antibody raised against the last nine amino acids of APP (Chemicon, Temecula CA, heretofore designed as CT9APP). In addition, the APP N-terminal fragments were detected with a 1:1500 dilution of 22C11 (Chemicon, Temecula, CA), which is specific for amino acids 66−81 of APP. Aβ peptides were detected with 6E10 (residues 1−17 of Aβ) and 4G8 (residues 17−24 of Aβ) using a 1:1500 dilution (Signet, Dedham, MA), as well as anti-Aβ 40 (0.5 μg/mL) and anti-Aβ 42 (0.5 μg/mL) (Biosource, Camarillo, CA). CT9APP, anti-Aβ 40, and anti-Aβ 42 antibodies were detected using a 1:10 000 dilution of goat anti-rabbit horseradish peroxidase (HRP)-conjugated secondary antibody from Pierce (Rockford, IL), and 22C11, 6E10, and 4G8 were incubated with 1:10 000-fold diluted goat anti-mouse HRP-conjugated antibody (Pierce, Rockford, IL). The Western blots were developed with SuperSignal West Pico Chemiluminescent Substrate and CL-Xpose film (Pierce, Rockford, IL) and Kodak GBX developer. All films were scanned using the GS-800 calibrated densitometer and analyzed with Quantity One software (Bio-Rad, Hercules, CA).

Immunoprecipitation of APP C-Terminal Fragments. A total of 100 μg of proteins from the formic acid-soluble 3−8-kDa FPLC fraction obtained from PDAPP Tg mice brains was used for the immunoprecipitation (IP). Formic acid was removed by drying under a speed vacuum and replacing it with 100 μL of distilled water. This procedure was repeated 3 times, and the resultant pellet was suspended in 1 mL of IP buffer: 30 mM Tris-HCl at pH 8 and 140 mM NaCl containing 0.1% Triton X-100 and the complete Protease Inhibitor Cocktail (Roche Diagnostics, Mannheim, Germany). This material was precleared by incubation with 5 μL of normal rabbit serum and Ultralink immobilized Protein A beads (Pierce, Rockford, IL) for 16 h at 4 °C followed by centrifugation at 3500 rpm for 5 min in an Eppendorf microfuge. The pellet was discarded, and the supernatant was incubated overnight at 4 °C with 5 μL of CT9APP (Chemicon, Temecula, CA) or rabbit antibody designated as 369 raised against the C-terminal 50 residues of APP (kindly provided by Dr. Sam Gandy) and 90 μL of a protein A beads slurry in IP buffer. After washing 3 times with IP buffer and 3 times with 10 mM Tris-HCl at pH 8, immunoprecipitates were suspended with an equal volume of 2× NuPAGE−LDS sample buffer (Invitrogen, Carlsbad, CA) containing 0.1 M DTT and boiled for 10 min. Proteins were analyzed by SDS−PAGE and Western blot with CT9APP (for 369 immunoprecipitates) and 369 antibodies (for CT9APP immunoprecipitates) as described in the previous section.

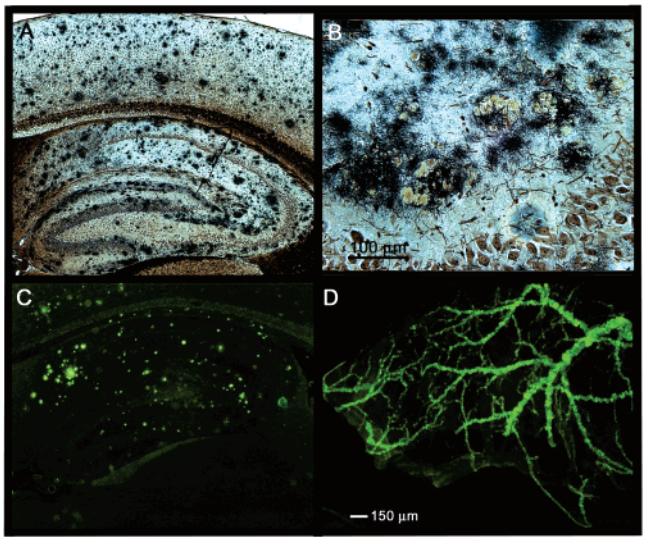

FIGURE 1: Sagital tissue sections of the 20-month-old PDAPP Tg mouse brain stained by silver and thioflavine-S. (A) Abundant number of amyloid plaques are stained by the Campbell−Switzer silver stain in the cortex and hippocampus of the PDAPP mouse. In some areas, the diffuse deposits are so numerous that the flocks of amyloid coalesced. Magnification at 25×. (B) At a larger magnification (200×), the diffuse amyloid deposits appear as flocculent conglomerates mixed with cellular conglomerates. (C) In a similar section to that shown in A, the thioflavine-S stained a limited number of amyloid deposits in the hippocampus and adjacent cortex. Magnification at 25×. (D) Tuft of PDAPP mouse parenchymal blood vessels demonstrating amyloid deposits stained with thioflavine-S. The brain tissue was removed by SDS−EDTA lysis. Magnification at 25×.

RESULTS

PDAPP Mouse Amyloid Deposit Biochemistry. In relation to the APP/Aβ metabolism, our experiments suggest that there are important differences between the PDAPP Tg mice model and sporadic AD. This strain of mice generated a large amount of flocculent amyloid plaques that accumulated with age and were clearly visible after Campbell−Switzer silver staining (parts A and B of Figure 1) and Aβ-immunocytochemistry procedures. However, unlike the amyloid plaques observed in sporadic AD, in the PDAPP mice, most of the plaques stained very faintly with thioflavine-S (Figure 1C) and were negative for Congo red birefringence. Although the abundant flocculent amyloid aggregates were completely dispersed in SDS−EDTA buffer, this material was recovered and concentrated by ultracentrifugation. In PDAPP mice, the number of plaques with dense amyloid cores exhibiting the intense thioflavine-S staining reaction was relatively low (Figure 1C), a characteristic that was also observed in the human V717F FAD specimens (*25*).

There was a mild to moderate amount of amyloid deposited in the PDAPP Tg mice vasculature at 20 months of age. This is a relative assertion because it is difficult to evaluate the amount of cerebrovascular amyloidosis in Tg

mice. In rodents, contrary to humans, some longitudinal vascular collagen fibers are intensely stained by thioflavine-S, a feature that can hamper an exact evaluation of vascular amyloidosis by fluorescence staining. In contrast, the deposits of Aβ are perpendicular to the main axis of the vessel. A view of a parenchymal PDAPP Tg mouse tuft of blood vessels is shown in Figure 1D. We isolated the blood vessel network from a pool of 12 PDAPP Tg mice by SDS−EDTA lysis of the brain parenchymal tissue, following the procedure described for the V717F FAD cases (*25*). Unfortunately, GDFA extraction and FPLC separation of this isolated vascular Aβ did not yield sufficient material for further characterization.

An attempt was made to isolate PDAPP Tg mice compact amyloid cores by lysis of the brain parenchyma with SDS−EDTA and enrichment by sucrose gradients, a method employed successfully to isolate the amyloid cores from brains affected with sporadic AD (*27*). These procedures failed for the Tg mice probably because of the fact that these amyloid cores are dispersed completely by the action of the detergent and chelating agent. However, in a parallel experiment with a human APP V717F FAD case sample, compact amyloid cores were successfully isolated using SDS−EDTA/sucrose gradients at the 1.5−1.7 M sucrose interface. In addition, abundant neurofibrillary tangles (NFT) were obtained at the 1.7−2.0 M sucrose interface from the FAD V717F case. The human FAD amyloid cores were subsequently purified by size-exclusion FPLC and reverse-phase HPLC at alkaline pH (5RPC column) that yielded a series of 15 discrete peaks. However, mass spectroscopy analysis demonstrated that the average and monoisotopic molecular masses of all of these peptides corresponded to Aβ 1−42, suggesting the presence of species with different electrostatic charges and polarities (data not shown). As is the case for sporadic AD, these peptides in all probability represent an assortment of isomeric molecules with iso-Asp at positions 1, 7, and 23. These structural alterations in the peptide backbone that increasingly accumulate with time result in β shifts that change the retention time of the Aβ peptides and allow their separation on reverse-phase HPLC (*27*). Thus, the peptides containing L-iso-Asp elute first, followed by those containing D-iso-Asp, L-Asp, and D-Asp, respectively. To demonstrate that the multiple FAD Aβ fractions separated by HPLC were not the product of artifactual molecular alterations caused by the formic acid treatment, synthetic Aβ 1−42 was acid-treated and chromatographed using exactly the same conditions employed for the FAD Aβ peptides. The elution profile consisted of only two peaks corresponding to Aβ 1−42 and Aβ 1−42 oxidized. Intriguingly, the Aβ peptides present in the compact and SDS-insoluble cores of FAD amyloid showed minimal degradations at the N terminus, which contrasts sharply with the shortened and ragged N termini of the Aβ peptides observed in sporadic AD. The morphological and thioflavine-S staining characteristics of the comparatively sparse compact cores of amyloid of the PDAPP Tg mice suggest the presence of filaments composed of Aβ 1−42 similar to those found in its FAD counterpart, although this could not be determined in the present study.

APP Processing in PDAPP Mice and Humans. Western blot experiments revealed that the metabolic processing of APP in the cortex appears to be very different among PDAPP

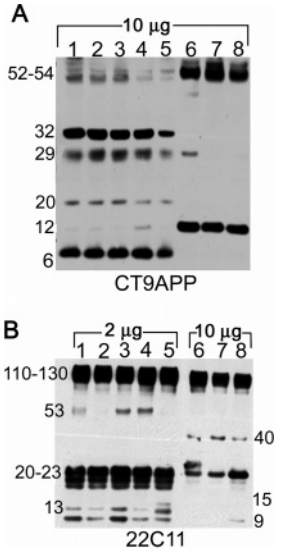

FIGURE 2: Western blots of PDAPP Tg mice (lanes 1−5) and human FAD (lane 6), sporadic AD (lane 7), and nondemented control (lane 8). The amount of protein (micrograms) loaded is indicated on the top of each gel. The apolipoprotein E genotypes for the human cases were ϵ3/ϵ3 (FAD), ϵ4/ϵ4 (sporadic AD), and ϵ3/ϵ3 (control nondemented). (A) Western blot developed with the CT9APP. The most prominent differences between mice and human were the presence of 32-, 20-, and 6-kDa bands in the former, which were missing in the human cases, and the nearly undetectable 10−12-kDa band, which corresponds to the C-terminal fragments CT99 and CT83 produced by the β- and α-secretases, respectively. The 29-kDa band was only seen in the FAD and Tg mice. (B) Western blot developed with the 22C11 antibody against the N-terminal domain of APP. Major differences in processing are also evident at the N-terminal region of the Tg mice when compared to the human.

Tg mice, human FAD (V717F), sporadic AD, and nondemented controls (Figure 2). Using the CT9APP antibody, heavy CT99 and CT83 fragment bands were present in humans (~10−12 kDa) that were almost absent in the PDAPP Tg mice. Bands were detected between 52 and 54 kDa in human FAD but were weak in PDAPP mice, while the mice had cross-reacting bands at 32, 20, and ~6 kDa, which were completely absent in the humans (Figure 2A). A 29-kDa band was common to the FAD case and the PDAPP Tg mice, although more apparent in the latter. Different fragments were also seen when using 22C11, an antibody recognizing the amino terminus of APP (Figure 2B). Some of the Tg mice possessed a 53-kDa band that was absent in humans, while the humans had a weak 40-kDa band that was not seen in the Tg mice. All samples contained bands between 20 and 23 kDa, but these were more evident in the PDAPP Tg mice. In addition, the mice had bands at 15, 13, and 9 kDa. Only the 9 kDa was barely detectable in the human ND control. Additional differences between FAD and the Tg mouse were also detected on Western blots probed with 6E10 (data not shown). This antibody identified in the PDAPP Tg mice a 29-kDa M_r fragment (~260 amino acids long). An analogous fragment was not present in the human brain homogenates. The same 29-kDa band, although fainter, was also detected by the 4G8 monoclonal antibody (data not shown). The 6E10 antibody (Aβ 1−17) identified a 58-kDa (~525 amino acids long) molecule, which carries the complete Aβ sequence within an internal APP peptide fragment.

PDAPP Tg Mice Aβ Peptide Structure. Mass spectrometry analysis by SELDI−TOF of the total PDAPP-Aβ-related peptides extracted by 80% GDFA, enriched by Superose 12 size-exclusion FPLC (Figure 3A), and purified by reverse-phase HPLC (Figure 3B), revealed that the 3−8 kDa fraction contained a complex assortment of Aβ-related peptides present in fractions 1−4. As can be noted in Table 1, the Aβ antibodies 6E10, 4G8, R293, and R306 captured Aβ-related peptides that in SELDI−TOF mass spectrometry suggested amino acid sequences with N termini at residues 1, 2, 3, 4, 7, 9, 10, 11, 13, 15, 16, 17, 32, and 33 and with C termini at positions 34, 35, 36, 37, 38, 39, 40, 41, 42, 43, 44, 45, 46, 47, 48, 51, 53, 54, 61, 62, and 64 (Aβ sequence notation). The PDAPP Aβ-related peptides, separated by reverse-phase HPLC (Figure 3B), were subsequently treated with trypsin and CNBr, and the resulting peptides were separated by reverse-phase HPLC at pH 2.0 (parts C−E of Figure 3). Mass spectrometry analysis by MALDI−TOF confirmed the presence of Aβ-related peptides and suggested N termini at positions 2, 3, 6, 17, 29, and 36 and C termini at positions 5, 16, 28, 40, 41, 42, 43, 45, 46, 47, 48, 49, 51, and 52 (Table 2). Interestingly, no peptide with the C-terminal at position 35 was found that may be explained as resulting from oxidation of Met that prevented CNBr cleavage. However, because there are numerous peptides with N termini at position 36 (see Table 2), it seems most likely that the CNBr cleavage probably occurred and we failed to detect molecules terminating at residue 35 (i.e., trypsin-CNBr Aβ residues 29−35, with the latter residue in the form of homoserine/homoserine lactone). The sensitivity of both SELDI−TOF and MALDI−TOF mass spectrometry also revealed numerous endogenous murine Aβ-related peptides carrying the rodent wild-type amino acids: Gly5, Phe10, Arg13, and Val at position 46 (data not shown). The molecular masses of the endogenous mouse Aβ peptides accounted for N termini starting at residues 1−20 and C termini ending at residues 34−55 (Aβ sequence notation). Figure 4 illustrates a SELDI−TOF spectrum accounting for Aβ peptides with C termini at residues 53Lys and 54Lys, which were captured by the 6E10 antibody in the HPLC peak number 4 (Figure 3B). These peptides were also independently captured, in the same HPLC fraction, by anti-Aβ antibodies 4G8, R293, and R306 (Table 1). All of the above sequences are given in the Aβ notation.

Immunoprecipitation. The FPLC formic acid-soluble, 3−8-kDa fraction was immunoprecipitated with CT9APP and analyzed by Western blot with polyclonal antibody 369. A strong band of ~6-kDa apparent M_r was detected that was not present in the negative controls (Figure 5A). When antibody 369 was used for immunoprecipitation and CT9APP for Western blot detection (Figure 5B), the same specific band was consistently seen, confirming its identity as a C-terminal fragment of APP that most likely included a sequence starting downstream of the γ-secretase site and the entire APP intracytoplasmic domain (Figure 6). Despite the sensitivity of the assay, no bands consistent with CT99 and CT83 APP fragments were detected. This result was in accordance with the Western blots of brain homogenates, in which bands compatible with CT99 and CT83 were clearly detected in the human samples only (Figure 2A).

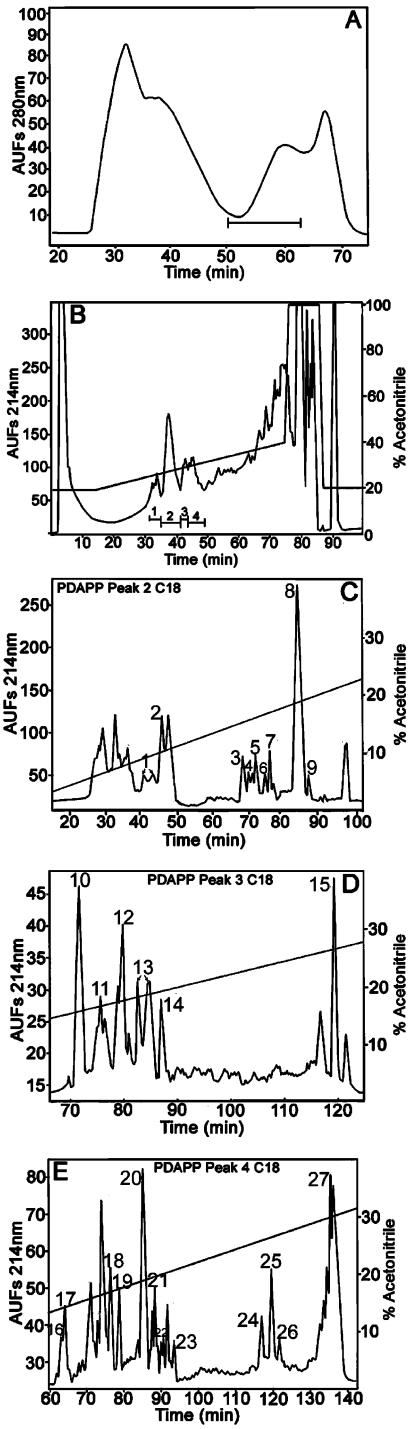

FIGURE 3: Chromatographic profiles of the PDAPP Tg mice Aβ peptides separated by FPLC and HPLC. (A) FPLC elution trace of the GDFA brain homogenates of PDAPP Tg mice. The acid-soluble fractions, underlined by a bar, eluted between 50 and 62 min and were pooled, and the volume was reduced. These fractions were submitted to HPLC (pH 2.0) reverse-phase column (C8, 80 °C), which was eluted with a linear acetonitrile gradient as shown in B. Fractions 1−4 contained the Aβ peptides. The amount of Aβ peptides contained in peak 1 was too small, and no further purification was carried out. Peaks 2, 3, and 4 were submitted to tryptic digestion and CNBr cleavage, and the resulting peptides were purified on a C18 reverse-phase column at 60 °C, as shown in C, D, and E, respectively. In each case, the slopes indicate the acetonitrile elution gradients. The numbers above the chromatographic peaks correspond to the MALDI−TOF mass spectra of peptides related to human Aβ, and their respective molecular masses are given in Table 2. The peaks not labeled correspond to endogenous mouse peptides.

Table 1: Human Aβ-Related Peptides Characterized by SELDI−TOF[a]

antibody/peak	observed M_r	calculated M_r	peptide	antibody/peak	observed M_r	calculated M_r	peptide
6E10/1	4149.6	4148.6	1−38 + O	4G8/4	3149.5	3150.8	17−47 (phe)
6E10/2	3163.2	3162.7	11PG−40 + f		3817.9	3817.4	4−38
	3272.4	3273.8	9−39			3820.3	2−35 + O
	4132.5	4132.6	1−38		4334.0	4330.0	4−43 + 2O
	7073.5	7069.2	1−64 (phe) + O			4330.0	7−47 (phe)
6E10/3	4075.0	4075.6	1−37			4330.9	1−40
	4132.5	4132.6	1−38		4534.5	4531.2	1−42 + O
	4231.9	4231.8	1−39			4533.2	2−43 + 2O
		4231.8	2−40 + O		5712.6	5713.7	3PG−54 (phe) + O
	4347.4	4345.0	3−42 + O		5744.1	5741.7	3PG−54 (phe) + f + O
		4346.9	1−40 + O		5775.0	5774.8	1−53 (phe)
	7093.0	7097.2	1−64 (phe) + f + O	R293/3	4731.1	4731.4	1−44 + O
6E10/4	3818.1	3817.4	4−38			4729.5	2−45 + O
		3820.3	2−35 + O		7081.7	7081.2	1−64 (phe) + f
	4333.0	4330.0	4−43 + 2O	R293/4	3828.8	3830.3	3PG−36 + O
		4330.0	7−47 (phe)			3829.5	10−45 + O
		4330.9	1−40		4333.5	4330.0	4−43 + 2O
	4348.8	4345.0	3−42 + O			4330.0	7−47 (phe)
		4346.9	1−40 + O			4330.9	1−40
	4533.7	4531.2	1−42 + O		4534.4	4531.2	1−42 + O
		4533.2	2−43 + 2O			4533.2	2−43 + 2O
	5711.1	5713.7	3PG−54 (phe) + O		5711.6	5713.7	3PG−54 (phe) + O
	5742.8	5741.7	3PG−54 (phe) + f + O		5743.7	5741.7	3PG−54 (phe) + f + O
	5773.0	5774.8	1−53 (phe)		5774.5	5774.8	1−53 (phe)
4G8/1	2909.4	2906.5	17−45 + O	R306/1	3274.1	3273.8	9−39
	3790.3	3788.2	1−34			3275.1	32−61 (phe)
		3788.3	4−37 + f	R306/2	3163.3	3162.7	11PG−40 + f
		3791.3	7−42 + 2O			3163.8	15−45 + O
	4533.9	4531.2	1−42 + O			3161.9	33−61 (phe)
		4533.2	2−43 + 2O			3165.8	16−46 (phe)
	5236.8	5233.9	1−48 (phe) + f + O		3274.1	3273.8	9−39
	5377.7	5372.2	3PG−51 (phe) + f + O			3275.1	32−61 (phe)
	6726.6	6724.8	3PG−62 (phe) + 2O		7092.8	7097.2	1−64 (phe) + f + O
4G8/2	3141.6	3140.7	13−42 + 2O	R306/3	4730.1	4729.5	2−45 + O
	3286.2	3281.9	11−41 + O			4731.4	1−44 + O
	4333.9	4330.0	4−43 + 2O		6153.7	6158.2	1−54 (phe)
		4330.0	7−47 (phe)		7092.8	7097.2	1−64 (phe) + f + O
		4330.9	1−40	R306/4	3827.2	3829.5	10−45 + O
	4518.5	4517.2	2−43 + O			3830.3	3PG−36 + O
		4518.4	10−51 (phe)		4532.7	4531.2	1−42 + O
	4719.9	4715.3	1−44			4533.2	2−43 + 2O
	7078.4	7081.2	1−64 (phe) + f		5709.6	5313.7	3PG−54 (phe) + O
4G8/3	4733.8	4731.4	1−44 + O		5740.7	5741.7	3PG−54 (phe) + f + O
		4729.5	2−45 + O		5770.2	5773.7	1−53 (phe)
	7092.5	7097.2	1−64 (phe) + f + O				

[a] PG, pyroglutamyl; f, +1 formyl (M_r, +28); 2f, +2 formyl (M_r, +56); O, +1 oxygen (M_r, +16); 2O, +2 oxygen (M_r, +32).

DISCUSSION

PDAPP Tg mice create an Aβ pathology reminiscent of sporadic AD, but both the underlying proteolytic mechanisms and the Aβ plaque morphology deviate substantially from those seen in virtually all AD patients. Western blots revealed that the PDGF promoter-driven expression of the APP V717F transgene yields approximately 10 times more translated protein than that observed in either AD cases or in nondemented human controls. The V717F FAD mutation, located 4−6 amino acids distal to the normal Aβ 40/42 C termini, results in massive Aβ peptide production coupled with an increased synthesis of Aβ42. PDAPP Tg mouse amyloid deposition can be evident as early as 6 months of age with the initial development of compact core amyloid plaques (*28*). After 12 months, there is a dramatic increase in the accumulation of flocculent amyloid deposits. At 20 months of age, PDAPP Tg mice have a florid and severe amyloid pathology in the cortex and hippocampus, mostly consisting of flocculent diffuse plaques that at times coalesce into sheetlike structures and a moderate number of thioflavine-S stainable core plaques (*28*). It has been widely assumed that diffuse plaques represent the initial deposits of Aβ, a sort of "pre-amyloid", which subsequently evolves into the amyloid core plaques. The sequence of events and the nature of the amyloid deposits in the PDAPP Tg mice endorse our earlier observation that diffuse plaques and compact amyloid plaques form independently (*29*). We were unable to obtain sufficient material to analyze PDAPP Tg mouse vascular amyloid. However, in the V717F FAD case, the leptomeningeal vascular amyloid was composed of Aβ peptides mostly starting at residues 1 and 2 and ending at residues 38, 39, 40, 42, and 44, with a lesser representation of shorter Aβ peptides ending at residues 22, 23, 24, 25, 26, 30, and 31 (*25*).

Our observations suggest that the bulk of the unusual Aβ peptides produced in the PDAPP Tg mice results from an aberrant γ-secretase activity combined with additional murine protease activities. The gross overload of APP and a murine-specific peptide degradation could explain the miscellaneous and profuse fragments found in PDAPP Tg mice, which are

Table 2: Human Tryptic and CNBr Aβ-Related Peptides Characterized by MALDI−TOF[a]

peak number	observed M_r	calculated M_r	peptide
5	1429.6	1429.9	36−49 (phe) + f
6	1429.7	1429.9	36−49 (phe) + f
8	955.5	955.6	36−45 + f
	1816.9	1817.1	36−52 (phe) + O + 2f
9	1816.8	1817.1	36−52 (phe) + O + 2f
10	1816.8	1817.1	36−52 (phe) + O + 2f
11	1074.5	1074.7	36−46 (phe)
	1800.8	1801.1	36−52 (phe) + 2f
	1816.8	1817.1	36−52 (phe) + O + 2f
12	1800.8	1801.1	36−52 (phe) + 2f
	1816.8	1817.1	36−52 (phe) + O + 2f
13	1325.7	1325.7	17−28
14	1325.6	1325.7	17−28
	1353.6	1353.7	17−28 + f
16	1816.8	1817.1	36−52 (phe) + O + 2f
	1870.8	1871.1	29−47 (phe) + f
17	1871.5	1871.1	29−47 (phe) + f
	1899.6	1899.1	29−47 (phe) + 2f
	2549.9	2549.4	17−41 + O + f
18	1198.6	1198.7	29−41
19	1325.7	1325.7	17−28
20	1353.8	1353.7	17−28+f
22	1364.6	1364.6	6−16+f
	3113.2	3113.5	3−28PG + 2f
24	430.2	430.3	36−40
	433.1	433.1	3−5PG
25	1750.8	1750.8	3−16PG
29	433.0	433.1	3−5PG
	451.2	451.1	3−5
30	1198.8	1198.7	29−41
31	1325.6	1325.7	17−28
32	1325.7	1325.7	17−28
33	2576.3	2576.4	17−42
35	1750.9	1750.8	3−16PG
36	433.1	433.1	3−5PG
	1364.8	1364.6	3−16 + f
	2303.6	2303.3	29−51 (phe) + O
	2343.6	2343.4	29−51 (phe) + 2f
37	1364.7	1364.6	3−16 + f
	2677.6	2677.5	17−43
	3113.7	3113.5	3−28PG + 2f
	3146.6	3146.5	2−28
38	433.1	433.1	3−5PG
	1631.9	1632.0	36−51 (phe)
	2677.7	2677.5	17−43
39	433.3	433.1	3−5PG

[a] PG, pyroglutamyl; f, +1 formyl (M_r, +28); 2f, +2 formyl (M_r, +56); O, +1 oxygen (M_r, +16); peaks 1, 2, 15, 21, 23, 34, and 40 did not exhibit assignable masses.

not present in the human brain homogenates. The recently published rodent genome describes several proteases which are without counterpart in humans (*30*). In addition, some experiments reveal that alternate APP-processing pathways exist and raise the possibility that mice express different precursor cleavage modes. For example, human skeletal muscle has the capacity to produce both Aβ 40/42 and extended amyloid peptides ending at residues 44, 45, and 46 (*31*). A similar finding has been reported in the cerebrospinal fluid of AD patients in which the elongated Aβ peptides 1−45 and 2−46 were detected (*32*). Furthermore, a new presenilin-dependent cleavage site has been localized in the APP molecule that corresponds to position 46 in the Aβ sequence and has been dubbed the ζ site (*33*). It is possible that, in the PDAPP Tg mice, the presence of the bulky benzene ring of Phe at position 46 impairs γ-secretase cleavage site recognition, thus altering production of classical

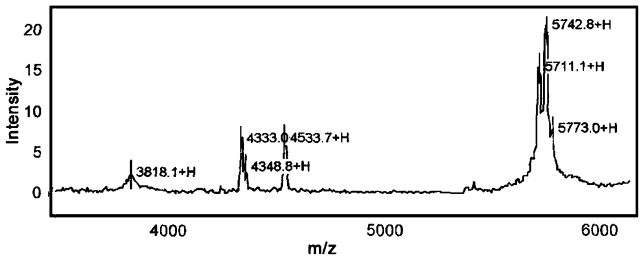

FIGURE 4: SELDI−TOF mass spectra profile of the PDAPP Tg mice using the monoclonal antibody 6E10 as the capture antibody. The molecular masses 5742.8, 5711.1, and 5773.0, corresponded to those of Aβ peptides: 3 (pyroglutamyl)−54 oxidized and formylated, 3 (pyroglutamyl)−54 oxidized, and 1−53, respectively. As shown in Table 1, these peptides were also captured by SELDI−TOF using the monoclonal antibody 4G8 and the polyclonal antibodies R293 and R306 raised against Aβ residues 34−40 and 36−42, respectively. All three peptides are in the human form of the APP transgene carrying the Phe mutation (instead of the wild-type Val) at position Aβ46.

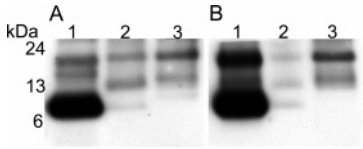

FIGURE 5: Western blots of the immunoprecipitated C-terminal peptide of the PDAPP Tg mice. (A) CT9APP immunoprecipitated band. Lane 1, PDAPP sample; lane 2, PDAPP negative control; and lane 3, CT9APP negative control. (B) 369 (CT50APP) immunoprecipitated band. Lane 1, PDAPP sample; lane 2, PDAPP negative control; and lane 3, 369 (CT50APP) negative control.

Aβ peptides. It is also possible that the PDAPP mouse γ-secretase was overwhelmed by the massive amounts (10-fold) of mutated APP and that this overabundant molecule pool was degraded by other endopeptidases and/or carboxypeptidases, resulting in an assortment of extended C-terminal Aβ peptides. Alternatively, perhaps most of the longer Aβ peptides were processed at the ϵ-cleavage site on the C side of residues Aβ48 and Aβ49 (*34*−*36*), which is dependent on α-secretase precutting. This may also explain the abundance of Aβ peptides starting at residue 17 in the PDAPP Tg mice (*37*, *38*). The ϵ cleavage generates the APP intracellular domains (AICD) of approximately 6 kDa containing residues 645−695 (*39*). It has been recently reported that γ-secretase, besides producing Aβ40 and Aβ42, can also generate longer forms of the Aβ peptides ending at Aβ43, Aβ45, Aβ46, and Aβ48, and these species have been identified within cells and brain tissue (*40*).

The increased solubility of the PDAPP Aβ, compared to the Aβ of sporadic AD, could be due to the comparative absence of post-translational modifications. Carboxy-terminus-extended Aβ peptides would become more hydrophobic because they contain extra nonpolar residues present in the transmembrane domain. However, the elongated Aβ sequences also contain some hydrophilic potential in the hydroxyl moieties of Thr43 and Thr48 and on the sulfone and/or sulfoxide forms of Met35. The polarity of elongated Aβ peptides may also be increased if they include the ϵ-amino groups of Lys53, Lys54, and Lys55. In addition, a looser folding of the elongated Aβ present in PDAPP mice may preclude a more stable hydrogen bonding as proposed for the AD amyloid (*41*, *42*). These changes would also explain the morphological features and staining character-

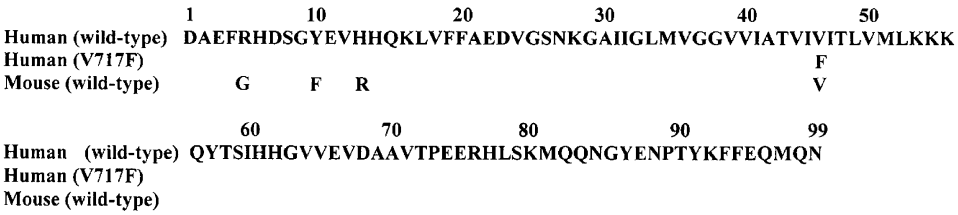

FIGURE 6: Amino acid sequences of the APP C-terminal domain human (wild type), human (V717F), and mouse (wild type) from residue Aβ 1 to the APP C terminus.

istics of the abundant flocculent diffuse plaques seen in both the FAD (V717F) (*25*) and PDAPP (V717F) Tg mice (*28*). Our data indicate that in the FAD V717F case the purified compact amyloid cores mainly contain SDS-insoluble and partially modified Aβ 1−42 and associated glycolipids and glycoproteins. These observations suggest that in the PDAPP Tg mice the analogous thioflavine-S positive amyloid cores may be composed of Aβ 1−42 that is more readily solubilized in the presence of detergents, whereas the abundant Aβ flocculent deposits are predominately elongated Aβ peptides.

We have characterized the chemical composition of the amorphous diffuse plaques in sporadic AD and found them to be mainly composed of the Aβ17−42 or P3 peptide (*29*). In humans, the fibrillar amyloid plaque cores are mainly made of Aβ 1−42 with a variable degree of degraded N termini and post-translationally modified peptides (*27*), while the vascular amyloid is chiefly composed of Aβ 1−40 with a lesser contribution of Aβ 1−42 (*43*). More recently, the existence of P3 in diffuse plaques and dystrophic neurites was confirmed and postulated to be a potential contributor to AD pathology (*29*, *44*−*49*). Interestingly, in Down's syndrome, the nonamyloidogenic P3 fragment is the major constituent of the diffuse cerebellar plaques (*46*). The lack of microgliosis around the diffuse Aβ deposits in AD could be due to the missing sequence of residues 1−16, which carries the HHQK motif (Aβ residues 13−16), necessary for the activation and secretion of microglia neurotoxic and pro-inflammatory molecules (*50*, *51*). In AD, the shorter Aβ 17−42 sequence organizes into amorphous water-insoluble aggregates with unique secondary and tertiary structures that differ from the fibrillar Aβ.

Amyloid-β deposits of sporadic AD, FAD V717F, and PDAPP Tg mice differ in chemical composition and critical physical characteristics, such as solubility and proteolytic vulnerability of the Aβ peptides. In sporadic AD, Aβ with pyroglutamyl at position 3 composes up to 50% of the total amyloid (*52*). The abundance of degraded N termini, representing up to 80% of the total amyloid (*27*), and the high proportion of isomerized Asp (iso-Asp) and racemized Asp and Ser residues (*27*) apparently confer to the Aβ of sporadic AD vastly greater insolubility (*53*) when compared to the Tg mice Aβ. Logarithmic regression curves obtained by plotting the time-dependent degree of Aβ oligomerization showed that Aβ 1−42 with iso-Asp at position 1 and 7 has the fastest rate of aggregation followed by Aβ 1−42 and Aβ 3-pyroglutamyl-42 (*53*). Under the same experimental conditions, the susceptibility of Aβ to trypsin digestion substantially decreased from 95% for Aβ 1−40 monomer, 57% for Aβ 1−42 monomer, 54% for Aβ 3-pyroglutamyl-42 monomer, 41% for Aβ 1−42 (iso-Asp 1, 7) monomer, 20% for 1−42 (iso-Asp 1, 7) dimer, and 2% for Aβ 17−42 monomer (*53*). Another important difference between human and Tg mice Aβ is the high proportion of irreversibly denatured Aβ dimers and tetramers present in the former, where they account for up to 40% of the total amyloid (*54*). We have demonstrated that these dimers and tetramers are efficient neuronal killers in the presence of microglia (*54*) and are present in negligible amounts in the APP Tg mice (*7*−*9*).

Striking differences also exist between the Aβ peptides produced by the PDAPP Tg mice compared to those generated in tg2576 and APP23 Tg mice (*8*, *9*). These two Tg mice carry the Swedish double mutations K670N and M671L (APP_{770} numbering), with the former inserted into the hamster Prion protein cosmid vector and the latter under the control of the neuron-specific mouse Thy-1 promoter. In these animals, the only Aβ peptides recovered by the same analytical methodology applied for the PDAPP Tg mice were Aβ1−37, Aβ1−38, Aβ1−39, Aβ1−40, and Aβ1−42, with a very small level of oxidized isoforms (*8*, *9*, *55*). Furthermore, Western blots of the tg2576 indicated the presence of abundant CT99 and CT83 (*9*), which were negligible in the PDAPP Tg mice, and an apparent absence of the ~6-kDa band, which was plentiful in the PDAPP Tg mice. The tg2576 and APP23 mice also differ from the PDAPP in amyloid plaque morphology and histochemistry and exhibit a profusion of large thioflavine-S positive amyloid plaques resembling those observed in AD while producing a relatively reduced number of diffuse plaques. In addition, the PDAPP Tg mice show a moderate amount of vascular amyloid deposits similar to those seen in the tg2576 Tg mice (*7*), while the APP23 has abundant amyloid loading in both the leptomeninges and cortical arteries (*7*). A relevant feature shown in APP Tg mice is that all amyloid plaques contain apolipoprotein E in amounts that correlate with the amyloid burden, suggesting that this molecule plays a role in amyloid deposition and clearance (*6*, *56*). Idiosyncratic differences in APP processing among the Tg mice strains complicate experimental interpretations and extrapolation to the human AD condition.

Overall, the Aβ structure and amyloid deposition pattern of the PDAPP Tg mice more closely resembles that of FAD cases carrying the APP V717F mutation (*25*), rather than those characteristic of sporadic AD. The accumulation of abundant soluble flocculent amyloid deposits in both FAD V717F cases and PDAPP Tg mice is probably due to the production of longer Aβ peptides, primarily because of a mutation that reduces γ-secretase cleavage efficiency and simultaneously creates substrates for alternative proteolytic pathways. Phenylalanine-scanning mutagenesis along the transmembrane region of APP-CT99 affects the interaction between this peptide and the γ-secretase, thus changing the specificity of the enzyme (*57*). Moreover, it has been reported

that about 30% of the APP C-terminal fragments are converted into Aβ by the action of the γ-secretase, and the remaining 70% are degraded by an alternative proteasome-dependent pathway (*58*). In sporadic AD, β-secretase protein and activity levels are moderately increased (*59*−*61*), contributing to the production of Aβ peptides. In PDAPP Tg mice, the increased generation of APP C-terminal fragments may elevate the caspase-mediated production of APP-CT31, a pro-apoptotic peptide that may add to brain pathology (*62*−*66*). Our chemical characterization of Aβ in humans and rodents (*6*−*9*, *11*, *25*, *27*, *29*, *42*, *43*, *52*−*54*, *67*−*73*) strongly suggests that there are important differences in the kinetics of filament formation between Tg mice and sporadic AD. In the case of the Tg mice, mutant APP genes driven by powerful promoters produce enormous quantities of Aβ peptides that overwhelm the clearance ability of the rodents and generate profuse amyloid deposits in a matter of months. In sporadic AD, the rate of Aβ synthesis remains at a steady state but the time-dependent accumulation of post-translational modifications catalyze filament formation and promote polymer stability over periods of 3−4 decades. This action is compounded by an age-dependent reduction in the enzymes that degrade Aβ (*74*−*78*). In humans, there is a time-dependent irreversible cross-linkage of Aβ dimers and tetramers that enhances insolubility and resistance to proteolytic degradation.

Immunization of APP Tg mice with Aβ or administration of anti-Aβ antibodies resulted in a reduction of the amyloid load in hippocampus and cerebral cortex and, more important, apparently reversed some cognitive deficiencies (*21*, *79*−*81*). Autopsy analyses suggest that an analogous removal of Aβ peptides occurs in vaccinated AD patients (*14*−*16*). Unfortunately, some patients unexpectedly developed meningoencephalitis, a complication that was not observed in the vaccinated Tg mice. It is important to consider that APP Tg mice differ from AD patients, and these differences may complicate the interpretation of human vaccination trials. Some APP Tg mice produce massive quantities of diverse peptides that create profuse amyloid deposits in a very short period of time. However, these summarily developed amyloid deposits lack the structural modifications and associated glycoproteins and glycolipids that are abundant in the Aβ peptides that accumulate over decades in the aging human brain. The relentless accumulation of undegradable Aβ elicits a sustained inflammatory reaction, mediated by activated microglia and probably by invading peripheral macrophages as well, that culminates in the release of cytokines, chemokines, and toxins that may injure neurons and glia, damage the vasculature, and breech the integrity of the blood-brain barrier (BBB). A similar deleterious biochemical effects cascade is either not present in Tg mice or, on the basis of vaccine-mediated cognitive function recovery, is not as pronounced in these animals. In all models in which Aβ vaccination was attempted, the vascular amyloid appears to be unaltered probably because of its different peptide conformation or interactions with extracellular matrix molecules that hinders IgG access. Because total Aβ peptide levels remain unaltered and APP processing continues unabated in some vaccinated mice (*21*, *22*), it is possible that potentially toxic soluble Aβ species cannot exit amyloid-choked vessels. An increase in vascular amyloid could be interpreted as a result of microglial attempts to unload phagocytized Aβ into the circulation. It is known that microglia can internalize fibrillar Aβ by phagocytosis (*82*) and that in the absence of intracellular degradation Aβ can be released into the surrounding space (*83*).

Despite some biochemical differences, the Tg mice models remain promising and practical venues to investigate novel AD treatment approaches. Studies of Tg mice and human AD patients have revealed conclusively that amyloid plaques are dynamic and amenable to ablation through pharmacological interventions, although both Tg mice and AD patients harbor vascular amyloid deposits that resist dispersal by existing immunologic therapeutic protocols. Although vascular amyloid deposits potentially represent an obstacle to complete amyloid removal, testing new broader spectrum immunological strategies in Tg mice that also target recalcitrant vascular species may provide crucial insight as to the efficacy of such therapies in AD patients. In addition, more sophisticated Tg animals expressing new AD gene combinations may enable a more faithful modeling of sporadic AD and provide superior experimental tools to evaluate therapeutic interventions. Understanding at the molecular level the nature of these important animal models will permit informed interpretations of experiments to be undertaken with the ultimate goal to manage or reverse the ravages of sporadic AD.

ACKNOWLEDGMENT

We express our gratitude to Dr. Sam Gandy for the gift of the 369 antibody against the C-terminal 50 amino acid residues of APP and to Dr. Pankaj Mehta for the donation of the R293 and R306 antibodies against the C-terminal regions of Aβ 40 and Aβ 42, respectively.

REFERENCES

1. Brookmeyer, R., Gray, S., and Kawas, C. (1998) Projections of Alzheimer's disease in the United States and the public health impact of delaying disease onset, *Am. J. Public Health 88*, 1337−1342.
2. Glenner, G. G., and Wong, C. W. (1984) Alzheimer's disease: Initial report of the purification and characterization of a novel cerebrovascular amyloid protein, *Biochem. Biophys. Res. Commun. 120*, 885−890.
3. Masters, C. L., Simms, G., Weinman, N. A., Multhaup, G., McDonald, B. L., and Beyreuther, K. (1985) Amyloid plaque core protein in Alzheimer disease and Down syndrome, *Proc. Natl. Acad. Sci. U.S.A. 82*, 4245−4249.
4. Hardy, J. A., and Higgins, G. A. (1992) Alzheimer's disease: The amyloid cascade hypothesis, *Science 256*, 184−185.
5. Selkoe, D. J. (2001) Alzheimer's disease results from the cerebral accumulation and cytotoxicity of amyloid β-protein, *J. Alzheimers Dis. 3*, 75−80.
6. Kuo, Y. M., Crawford, F., Mullan, M., Kokjohn, T. A., Emmerling, M. R., Weller, R. O., and Roher, A. E. (2000) Elevated Aβ and apolipoprotein E in AβPP transgenic mice and its relationship to amyloid accumulation in Alzheimer's disease, *Mol. Med. 6*, 430−439.
7. Kuo, Y. M., Beach, T. G., Sue, L. I., Scott, S., Layne, K. J., Kokjohn, T. A., Kalback, W. M., Luehrs, D. C., Vishnivetskaya, T. A., Abramowski, D., Sturchler-Pierrat, C., Staufenbiel, M., Weller, R. O., and Roher, A. E. (2001) The evolution of Aβ peptide burden in the APP23 transgenic mice: Implications for Aβ deposition in Alzheimer disease, *Mol. Med. 7*, 609−618.
8. Kuo, Y. M., Kokjohn, T. A., Beach, T. G., Sue, L. I., Brune, D., Lopez, J. C., Kalback, W. M., Abramowski, D., Sturchler-Pierrat, C., Staufenbiel, M., and Roher, A. E. (2001) Comparative analysis of amyloid-β chemical structure and amyloid plaque morphology of transgenic mouse and Alzheimer's disease brains, *J. Biol. Chem. 276*, 12991−12998.

9. Kalback, W., Watson, M. D., Kokjohn, T. A., Kuo, Y. M., Weiss, N., Luehrs, D. C., Lopez, J., Brune, D., Sisodia, S. S., Staufenbiel, M., Emmerling, M., and Roher, A. E. (2002) APP transgenic mice Tg2576 accumulate Aβ peptides that are distinct from the chemically modified and insoluble peptides deposited in Alzheimer's disease senile plaques, *Biochemistry 41*, 922−928.
10. Schwab, C., Hosokawa, M., and McGeer, P. L. (2004) Transgenic mice overexpressing amyloid β protein are an incomplete model of Alzheimer disease, *Exp. Neurol. 188*, 52−64.
11. Roher, A. E., and Kokjohn, T. A. (2003) Appraisal of AβPP transgenic mice as models for Alzheimer's disease, *Curr. Med. Chem. 3*, 85−90.
12. Schenk, D., Barbour, R., Dunn, W., Gordon, G., Grajeda, H., Guido, T., Hu, K., Huang, J., Johnson-Wood, K., Khan, K., Kholodenko, D., Lee, M., Liao, Z., Lieberburg, I., Motter, R., Mutter, L., Soriano, F., Shopp, G., Vasquez, N., Vandevert, C., Walker, S., Wogulis, M., Yednock, T., Games, D., and Seubert, P. (1999) Immunization with amyloid-β attenuates Alzheimer-disease-like pathology in the PDAPP mouse, *Nature 400*, 173−177.
13. Arendash, G. W., Gordon, M. N., Diamond, D. M., Austin, L. A., Hatcher, J. M., Jantzen, P., DiCarlo, G., Wilcock, D., and Morgan, D. (2001) Behavioral assessment of Alzheimer's transgenic mice following long-term Aβ vaccination: Task specificity and correlations between Aβ deposition and spatial memory, *DNA Cell Biol. 20*, 737−744.
14. Nicoll, J. A., Wilkinson, D., Holmes, C., Steart, P., Markham, H., and Weller, R. O. (2003) Neuropathology of human Alzheimer disease after immunization with amyloid-β peptide: A case report, *Nat. Med. 9*, 448−452.
15. Ferrer, I., Boada, R. M., Sanchez Guerra, M. L., Rey, M. J., and Costa-Jussa, F. (2004) Neuropathology and pathogenesis of encephalitis following amyloid-β immunization in Alzheimer's disease, *Brain Pathol. 14*, 11−20.
16. Masliah, E., Hansen, L., Adame, A., Crews, L., Bard, F., Lee, C., Seubert, P., Games, D., Kirby, L., and Schenk, D. (2005) Aβ vaccination effects on plaque pathology in the absence of encephalitis in Alzheimer disease, *Neurology 64*, 129−131.
17. Hock, C., Konietzko, U., Streffer, J. R., Tracy, J., Signorell, A., Muller-Tillmanns, B., Lemke, U., Henke, K., Moritz, E., Garcia, E., Wollmer, M. A., Umbricht, D., de Quervain, D. J., Hofman, M., Maddalena, A., Papassotiropoulos, A., and Nitsch, R. M. (2003) Antibodies against β-amyloid slow cognitive decline in Alzheimer's disease, *Neuron 38*, 547−554.
18. Dodart, J. C., Bales, K. R., Gannon, K. S., Greene, S. J., DeMattos, R. B., Mathis, C., DeLong, C. A., Wu, S., Wu, X., Holtzman, D. M., and Paul, S. M. (2002) Immunization reverses memory deficits without reducing brain Aβ burden in Alzheimer's disease model, *Nat. Neurosci. 5*, 452−457.
19. DeMattos, R. B., Bales, K. R., Cummins, D. J., Dodart, J. C., Paul, S. M., and Holtzman, D. M. (2001) Peripheral anti-Aβ antibody alters CNS and plasma Aβ clearance and decreases brain Aβ burden in a mouse model of Alzheimer's disease, *Proc. Natl. Acad. Sci. U.S.A. 98*, 8850−8855.
20. DeMattos, R. B., Bales, K. R., Cummins, D. J., Paul, S. M., and Holtzman, D. M. (2002) Brain to plasma amyloid-β efflux: A measure of brain amyloid burden in a mouse model of Alzheimer's disease, *Science 295*, 2267.
21. Janus, C., Pearson, J., McLaurin, J., Mathews, P. M., Jiang, Y., Schmidt, S. D., Chishti, M. A., Horne, P., Heslin, D., French, J., Mount, H. T., Nixon, R. A., Mercken, M., Bergeron, C., Fraser, P. E., George-Hyslop, P., and Westaway, D. (2000) A β peptide immunization reduces behavioural impairment and plaques in a model of Alzheimer's disease, *Nature 408*, 979−982.
22. Wilcock, D. M., Rojiani, A., Rosenthal, A., Subbarao, S., Freeman, M. J., Gordon, M. N., and Morgan, D. (2004) Passive immunotherapy against Aβ in aged APP-transgenic mice reverses cognitive deficits and depletes parenchymal amyloid deposits in spite of increased vascular amyloid and microhemorrhage, *J. Neuroinflammation 1*, 24−35.
23. Winkler, D. T., Bondolfi, L., Herzig, M. C., Jann, L., Calhoun, M. E., Wiederhold, K. H., Tolnay, M., Staufenbiel, M., and Jucker, M. (2001) Spontaneous hemorrhagic stroke in a mouse model of cerebral amyloid angiopathy, *J. Neurosci. 21*, 1619−1627.
24. Murrell, J., Farlow, M., Ghetti, B., and Benson, M. D. (1991) A mutation in the amyloid precursor protein associated with hereditary Alzheimer's disease, *Sci. 254*, 97−99.
25. Roher, A. E., Kokjohn, T. A., Esh, C., Weiss, N., Childress, J., Kalback, W., Luehrs, D. C., Lopez, J., Brune, D., Kuo, Y. M., Farlow, M., Murrell, J., Vidal, R., and Ghetti, B. (2004) The human amyloid-β precursor protein$_{770}$ mutation 717 Val-Phe generates peptides longer than Aβ 40−42 and flocculent amyloid aggregates, *J. Biol. Chem. 279*, 5829−5836.
26. Mucke, L., Masliah, E., Yu, G. Q., Mallory, M., Rockenstein, E. M., Tatsuno, G., Hu, K., Kholodenko, D., Johnson-Wood, K., and McConlogue, L. (2000) High-level neuronal expression of Aβ 1−42 in wild-type human amyloid protein precursor transgenic mice: Synaptotoxicity without plaque formation, *J. Neurosci. 20*, 4050−4058.
27. Roher, A. E., Lowenson, J. D., Clarke, S., Wolkow, C., Wang, R., Cotter, R. J., Reardon, I. M., Zurcher-Neely, H. A., Heinrikson, R. L., Ball, M. J., and Greenberg, B. D. (1993) Structural alterations in the peptide backbone of β-amyloid core protein may account for its deposition and stability in Alzheimer's disease, *J. Biol. Chem. 268*, 3072−3083.
28. Reilly, J. F., Games, D., Rydel, R. E., Freedman, S., Schenk, D., Young, W. G., Morrison, J. H., and Bloom, F. E. (2003) Amyloid deposition in the hippocampus and entorhinal cortex: Quantitative analysis of a transgenic mouse model, *Proc. Nat. Acad. Sci. U.S.A. 100*, 4837−4842.
29. Gowing, E., Roher, A. E., Woods, A. S., Cotter, R. J., Chaney, M., Little, S. P., and Ball, M. J. (1994) Chemical characterization of A β 17−42 peptide, a component of diffuse amyloid deposits of Alzheimer disease, *J. Biol. Chem. 269*, 10987−10990.
30. Puente, X. S., and Lopez-Otin, C. (2004) A genomic analysis of rat proteases and protease inhibitors, *Genome Res. 14*, 609−622.
31. Kuo, Y. M., Kokjohn, A., Watson, M. D., Woods, A. S., Cotter, R. J., Sue, L. I., Kalback, W. M., Emmerling, M. R., Beach, T. G., and Roher, A. E. (2000) Elevated Aβ42 in skeletal muscle of Alzheimer disease patients suggests peripheral alterations of AβPP metabolism, *Am. J. Pathol. 156*, 797−805.
32. Lewczuk, P., Esselmann, H., Meyer, M., Wollscheid, V., Neumann, M., Otto, M., Maler, J. M., Ruther, E., Kornhuber, J., and Wiltfang, J. (2003) The amyloid-β (Aβ) peptide pattern in cerebrospinal fluid in Alzheimer's disease: Evidence of a novel carboxyterminally elongated Aβ peptide, *Rapid Commun. Mass Spectrom. 17*, 1291−1296.
33. Zhao, G., Mao, G., Tan, J., Dong, Y., Cui, M. Z., Kim, S. H., and Xu, X. (2004) Identification of a new presenilin-dependent ζ-cleavage site within the transmembrane domain of amyloid precursor protein, *J. Biol. Chem. 279*, 50647−50650.
34. Weidemann, A., Eggert, S., Reinhard, F. B., Vogel, M., Paliga, K., Baier, G., Masters, C. L., Beyreuther, K., and Evin, G. (2002) A novel ε-cleavage within the transmembrane domain of the Alzheimer amyloid precursor protein demonstrates homology with Notch processing, *Biochemistry 41*, 2825−2835.
35. Sato, T., Dohmae, N., Qi, Y., Kakuda, N., Misonou, H., Mitsumori, R., Maruyama, H., Koo, E. H., Haass, C., Takio, K., Morishima-Kawashima, M., Ishiura, S., and Ihara, Y. (2003) Potential link between amyloid β-protein 42 and C-terminal fragment γ 49−99 of β-amyloid precursor protein, *J. Biol. Chem. 278*, 24294−24301.
36. Eggert, S., Paliga, K., Soba, P., Evin, G., Masters, C. L., Weidemann, A., and Beyreuther, K. (2004) The proteolytic processing of the amyloid precursor protein gene family members APLP-1 and APLP-2 involves α-, β-, γ-, and ε-like cleavages: Modulation of APLP-1 processing by N-glycosylation, *J. Biol. Chem. 279*, 18146−18156.
37. Kametani, F. (2004) Secretion of long Aβ-related peptides processed at ε-cleavage site is dependent on the α-secretase precutting, *FEBS Lett. 570*, 73−76.
38. Kume, H., Maruyama, H., and Kametani, F. (2004) Intracellular domain generation of amyloid precursor protein by ε-cleavage depends on C-terminal fragment by α-secretase cleavage, *Int. J. Mol. Med. 13*, 121−125.
39. Funamoto, S., Morishima-Kawashima, M., Tanimura, Y., Hirotani, N., Saido, T. C., and Ihara, Y. (2004) Truncated carboxyl-terminal fragments of β-amyloid precursor protein are processed to amyloid β-proteins 40 and 42, *Biochemistry 43*, 13532−13540.
40. Qi-Takahara, Y., Morishima-Kawashima, M., Tanimura, Y., Dolios, G., Hirotani, N., Horikoshi, Y., Kametani, F., Maeda, M., Saido, T. C., Wang, R., and Ihara, Y. (2005) Longer forms of amyloid β protein: Implications for the mechanism of intramembrane cleavage by γ-secretase, *J. Neurosci. 25*, 436−445.
41. Lansbury, P. T., Jr., Costa, P. R., Griffiths, J. M., Simon, E. J., Auger, M., Halverson, K. J., Kocisko, D. A., Hendsch, Z. S., Ashburn, T. T., and Spencer, R. G. (1995) Structural model for

the β-amyloid fibril based on interstrand alignment of an antiparallel-sheet comprising a C-terminal peptide, *Nat. Struct. Biol. 2*, 990−998.
42. Chaney, M. O., Webster, S. D., Kuo, Y. M., and Roher, A. E. (1998) Molecular modeling of the Aβ-42 peptide from Alzheimer's disease, *Protein Eng. 11*, 761−767.
43. Lue, L. F., Kuo, Y. M., Roher, A. E., Brachova, L., Shen, Y., Sue, L., Beach, T., Kurth, J. H., Rydel, R. E., and Rogers, J. (1999) Soluble amyloid-β peptide concentration as a predictor of synaptic change in Alzheimer's disease, *Am. J. Pathol. 155*, 853−862.
44. Kida, E., Wisniewski, K. E., and Wisniewski, H. M. (1995) Early amyloid-β deposits show different immunoreactivity to the amino- and carboxy-terminal regions of β-peptide in Alzheimer's disease and Down's syndrome brain, *Neurosci. Lett. 193*, 105−108.
45. Higgins, L. S., Murphy, G. M., Jr., Forno, L. S., Catalano, R., and Cordell, B. (1996) P3 β-amyloid peptide has a unique and potentially pathogenic immunohistochemical profile in Alzheimer's disease brain, *Am. J. Pathol. 149*, 585−596.
46. Lalowski, M., Golabek, A., Lemere, C. A., Selkoe, D. J., Wisniewski, H. M., Beavis, R. C., Frangione, B., and Wisniewski, T. (1996) The "nonamyloidogenic" p3 fragment (amyloid β17−42) is a major constituent of Down's syndrome cerebellar preamyloid, *J. Biol. Chem. 271*, 33623−33631.
47. Tekirian, T. L., Saido, T. C., Markesbery, W. R., Russell, M. J., Wekstein, D. R., Patel, E., and Geddes, J. W. (1998) N-terminal heterogeneity of parenchymal and cerebrovascular Aβ deposits, *J. Neuropathol. Exp. Neurol. 57*, 76−94.
48. Szczepanik, A. M., Rampe, D., and Ringheim, G. E. (2001) Amyloid-β peptide fragments p3 and p4 induce pro-inflammatory cytokine and chemokine production *in vitro* and *in vivo*, *J. Neurochem. 77*, 304−317.
49. Wei, W., Norton, D. D., Wang, X., and Kusiak, J. W. (2002) Aβ 17−42 in Alzheimer's disease activates JNK and caspase-8 leading to neuronal apoptosis, *Brain 125*, 2036−2043.
50. Giulian, D., Haverkamp, L., Yu, J., Karshin, W., Tom, D., Li, J., Kirkpatrick, J., Kuo, Y. M., and Roher, A. E. (1996) Specific domains of β-amyloid from Alzheimer's plaque elicit neuron killing in human microglia, *J. Neurosci. 16*, 6021−6037.
51. Giulian, D., Haverkamp, L. J., Yu, J., Karshin, W., Tom, D., Li, J., Kazanskaia, A., Kirkpatrick, J., and Roher, A. E. (1998) The HHQK domain of β-amyloid provides a structural basis for the immunopathology of Alzheimer's disease, *J. Biol. Chem. 273*, 29719−29726.
52. Kuo, Y. M., Emmerling, M. R., Woods, A. S., Cotter, R. J., and Roher, A. E. (1997) Isolation, chemical characterization, and quantitation of Aβ 3-pyroglutamyl peptides from neuritic plaques and vascular amyloid deposits, *Biochem. Biophys. Res. Commun. 237*, 188−191.
53. Kuo, Y. M., Webster, S., Emmerling, M. R., DeLima, N., and Roher, A. E. (1998) Irreversible dimerization/tetramerization and post-translational modifications inhibit proteolytic degradation of Aβ peptides of Alzheimer's disease, *Biochim. Biophys. Acta 1406*, 291−298.
54. Roher, A. E., Chaney, M. O., Kuo, Y. M., Webster, S. D., Stine, W. B., Haverkamp, L. J., Woods, A. S., Cotter, R. J., Tuohy, J. M., Krafft, G. A., Bonnell, B. S., and Emmerling, M. R. (1996) Morphology and toxicity of Aβ (1−42) dimer derived from neuritic and vascular amyloid deposits of Alzheimer's disease, *J. Biol. Chem. 271*, 20631−20635.
55. Stoeckli, M., Staab, D., Staufenbiel, M., Wiederhold, K. H., and Signor, L. (2002) Molecular imaging of amyloid β peptides in mouse brain sections using mass spectrometry, *Anal. Biochem. 311*, 33−39.
56. Bales, K. R., Verina, T., Cummins, D. J., Du, Y., Dodel, R. C., Saura, J., Fishman, C. E., DeLong, C. A., Piccardo, P., Petegnief, V., Ghetti, B., and Paul, S. M. (1999) Apolipoprotein E is essential for amyloid deposition in the APP(V717F) transgenic mouse model of Alzheimer's disease, *Proc. Natl. Acad. Sci. U.S.A. 96*, 15233−15238.
57. Lichtenthaler, S. F., Wang, R., Grimm, H., Uljon, S. N., Masters, C. L., and Beyreuther, K. (1999) Mechanism of the cleavage specificity of Alzheimer's disease γ-secretase identified by phenylalanine-scanning mutagenesis of the transmembrane domain of the amyloid precursor protein, *Proc. Natl. Acad. Sci. U.S.A. 96*, 3053−3058.
58. Nunan, J., Shearman, M. S., Checler, F., Cappai, R., Evin, G., Beyreuther, K., Masters, C. L., and Small, D. H. (2001) The C-terminal fragment of the Alzheimer's disease amyloid protein precursor is degraded by a proteasome-dependent mechanism distinct from γ-secretase, *Eur. J. Biochem. 268*, 5329−5336.
59. Holsinger, R. M., McLean, C. A., Beyreuther, K., Masters, C. L., and Evin, G. (2002) Increased expression of the amyloid precursor β-secretase in Alzheimer's disease, *Ann. Neurol. 51*, 783−786.
60. Fukumoto, H., Cheung, B. S., Hyman, B. T., and Irizarry, M. C. (2002) β-Secretase protein and activity are increased in the neocortex in Alzheimer disease, *Arch. Neurol. 59*, 1381−1389.
61. Li, R., Lindholm, K., Yang, L. B., Yue, X., Citron, M., Yan, R., Beach, T., Sue, L., Sabbagh, M., Cai, H., Wong, P., Price, D., and Shen, Y. (2004) Amyloid β peptide load is correlated with increased β-secretase activity in sporadic Alzheimer's disease patients, *Proc. Natl. Acad. Sci. U.S.A. 101*, 3632−3637.
62. Weidemann, A., Paliga, K., Durrwang, U., Reinhard, F. B., Schuckert, O., Evin, G., and Masters, C. L. (1999) Proteolytic processing of the Alzheimer's disease amyloid precursor protein within its cytoplasmic domain by caspase-like proteases, *J. Biol. Chem. 274*, 5823−5829.
63. Pellegrini, L., Passer, B. J., Tabaton, M., Ganjei, J. K., and D'Adamio, L. (1999) Alternative, non-secretase processing of Alzheimer's β-amyloid precursor protein during apoptosis by caspase-6 and -8, *J. Biol. Chem. 274*, 21011−21016.
64. LeBlanc, A., Liu, H., Goodyer, C., Bergeron, C., and Hammond, J. (1999) Caspase-6 role in apoptosis of human neurons, amyloidogenesis, and Alzheimer's disease, *J. Biol. Chem. 274*, 23426−23436.
65. Lu, D. C., Rabizadeh, S., Chandra, S., Shayya, R. F., Ellerby, L. M., Ye, X., Salvesen, G. S., Koo, E. H., and Bredesen, D. E. (2000) A second cytotoxic proteolytic peptide derived from amyloid β-protein precursor, *Nat. Med. 6*, 397−404.
66. Lu, D. C., Soriano, S., Bredesen, D. E., and Koo, E. H. (2003) Caspase cleavage of the amyloid precursor protein modulates amyloid β-protein toxicity, *J. Neurochem. 87*, 733−741.
67. Roher, A., Wolfe, D., Palutke, M., and KuKuruga, D. (1986) Purification, ultrastructure, and chemical analysis of Alzheimer disease amyloid plaque core protein, *Proc. Natl. Acad. Sci. U.S.A. 83*, 2662−2666.
68. Roher, A. E., Palmer, K. C., Chau, V., and Ball, M. J. (1988) Isolation and chemical characterization of Alzheimer's disease paired helical filament cytoskeletons: Differentiation from amyloid plaque core protein, *J. Cell Biol. 107*, 2703−2716.
69. Roher, A. E., Palmer, K. C., Yurewicz, E. C., Ball, M. J., and Greenberg, B. D. (1993) Morphological and biochemical analyses of amyloid plaque core proteins purified from Alzheimer disease brain tissue, *J. Neurochem. 61*, 1916−1926.
70. Kuo, Y. M., Emmerling, M. R., Vigo-Pelfrey, C., Kasunic, T., Kirkpatrick, J. B., Murdoch, G. H., Ball, M. J., and Roher, A. E. (1996) Water-soluble Aβ (N-40, N-42) oligomers in normal and Alzheimer disease brains, *J. Biol. Chem. 271*, 4077−4081.
71. Kuo, Y. M., Emmerling, M. R., Bisgaier, C. L., Essenburg, A. D., Lampert, H. C., Drumm, D., and Roher, A. E. (1998) Elevated low-density lipoprotein in Alzheimer's disease correlates with brain Aβ 1−42 levels, *Biochem. Biophys. Res. Commun. 252*, 711−715.
72. Roher, A. E., Baudry, J., Chaney, M. O., Kuo, Y. M., Stine, W. B., and Emmerling, M. R. (2000) Oligomerization and fibril assembly of the amyloid-β protein, *Biochim. Biophys. Acta 1502*, 31−43.
73. Roher, A. E., and Kokjohn, T. A. (2002) Of mice and men: The relevance of transgenic mice Aβ immunizations to Alzheimer's disease, *J. Alzheimer's Dis. 4*, 431−434.
74. Morelli, L., Bulloj, A., Leal, M. C., and Castano, E. M. (2005) Amyloid β degradation: A challenging task for brain peptidases, *Subcell. Biochem. 38*, 129−145.
75. Caccamo, A., Oddo, S., Sugarman, M. C., Akbari, Y., and LaFerla, F. M. (2005) Age- and region-dependent alterations in Aβ-degrading enzymes: Implications for Aβ-induced disorders, *Neurobiol. Aging 26*, 645−654.
76. Nalivaevaa, N. N., Fisk, L., Kochkina, E. G., Plesneva, S. A., Zhuravin, I. A., Babusikova, E., Dobrota, D., and Turner, A. J. (2004) Effect of hypoxia/ischemia and hypoxic preconditioning/reperfusion on expression of some amyloid-degrading enzymes, *Ann. N. Y. Acad. Sci. 1035*, 21−33.
77. Morelli, L., Llovera, R. E., Mathov, I., Lue, L. F., Frangione, B., Ghiso, J., and Castano, E. M. (2004) Insulin-degrading enzyme in brain microvessels: Proteolysis of amyloid {β} vasculotropic variants and reduced activity in cerebral amyloid angiopathy, *J. Biol. Chem. 279*, 56004−56013.

78. Farris, W., Mansourian, S., Chang, Y., Lindsley, L., Eckman, E. A., Frosch, M. P., Eckman, C. B., Tanzi, R. E., Selkoe, D. J., and Guenette, S. (2003) Insulin-degrading enzyme regulates the levels of insulin, amyloid β-protein, and the β-amyloid precursor protein intracellular domain *in vivo*, *Proc. Natl. Acad. Sci. U.S.A. 100*, 4162−4167.
79. Higgins, G. A., and Jacobsen, H. (2003) Transgenic mouse models of Alzheimer's disease: Phenotype and application, *Behav. Pharmacol. 14*, 419−438.
80. Davis, S., and Laroche, S. (2003) What can rodent models tell us about cognitive decline in Alzheimer's disease? *Mol. Neurobiol. 27*, 249−276.
81. Morgan, D. (2003) Learning and memory deficits in APP transgenic mouse models of amyloid deposition, *Neurochem. Res. 28*, 1029−1034.
82. Paresce, D. M., Chung, H., and Maxfield, F. R. (1997) Slow degradation of aggregates of the Alzheimer's disease amyloid β-protein by microglial cells, *J. Biol. Chem. 272*, 29397.
83. Chung, H., Brazil, M. I., Soe, T. T., and Maxfield, F. R. (1999) Uptake, degradation, and release of fibrillar and soluble forms of Alzheimer's amyloid β-peptide by microglial cells, *J. Biol. Chem. 274*, 32301−32308.

BI051213+